3D Stochastic Geometry Model for Large-Scale Molecular Communication Systems

Yansha Deng*, Adam Noel†, Weisi Guo‡, Arumugam Nallanathan*, and Maged Elkashlan§
*Department of Informatics, King's College London, UK
† School of Electrical Engineering and Computer Science, University of Ottawa, Canada
‡ School of Engineering, University of Warwick, UK
§ School of Electronic Engineering and Computer Science, Queen Mary University of London, UK

arXiv:1605.08311v2 [cs.IT] 3 Aug 2016

***Abstract*—Information delivery using chemical molecules is an integral part of biology at multiple distance scales and has attracted recent interest in bioengineering and communication. The collective signal strength at the receiver (i.e., the expected number of observed molecules inside the receiver), resulting from a large number of transmitters at random distances (e.g., due to mobility), can have a major impact on the reliability and efficiency of the molecular communication system. Modeling the collective signal from multiple diffusion sources can be computationally and analytically challenging. In this paper, we present the first tractable analytical model for the collective signal strength due to randomly-placed transmitters, whose positions are modelled as a homogeneous Poisson point process in three-dimensional (3D) space. By applying stochastic geometry, we derive analytical expressions for the expected number of observed molecules at a fully absorbing receiver and a passive receiver. Our results reveal that the collective signal strength at both types of receivers increases proportionally with increasing transmitter density. The proposed framework dramatically simplifies the analysis of large-scale molecular systems in both communication and biological applications.**

***Index Terms*—molecular communications, absorbing receiver, passive receiver, stochastic geometry, interference modeling.**

I. Introduction

Molecular communication via diffusion has attracted significant bioengineering and communication engineering research interest in recent years [1]. Messages are delivered via molecules undergoing random walks [2], a prevalent phenomenon in biology [3]. In fact, molecular communication exists in nature at both the nano- and macro-scales, offering transmit energy and signal propagation advantages over wave-based communications [4, 5]. One application example is that swarms of nano-robots can track specific targets, such as a tumour cells, to perform operations such as targeted drug delivery [6]. In order to do so, energy efficient and tether-less communications between the nano-robots must be established in biological conditions [7], and possibly additional nano-bio-interfaces need to be implemented [8].

Fundamentally, molecular communications involves modulating information onto the property of a single or a group of molecules (e.g., number, type, emission time). When modulating the number of molecules, each messenger node will transmit information-bearing molecules via chemical pulses. In a realistic environment with a swarm of robots (i.e., messenger nodes) operating together, they are likely to transmit molecular messages simultaneously. Due to limitations in transmitter design and molecule type availability, it is likely that many transmitters will transmit the same type of information molecule. Thus, it is important to model the collective signal strength due to all transmitters with the same type of information molecule, and to account for random transmitter locations due to mobility.

Existing works have largely focused on modeling: 1) the signal strength of a point-to-point communication channel by considering the self-interference that arises from adjacent symbols (i.e., inter-symbol-interference (ISI)) at a passive receiver [9], at a fully absorbing receiver [10], and at a reversible adsorption receiver [11]; and 2) the collective signal strength of a multi-access communication channel at the passive receiver due to co-channel transmitters (i.e., transmitters emitting the same type of molecule) with the given knowledge of their total number and location [9].

The first work to consider randomly distributed co-channel transmitters in 3-D space according to a spatial homogeneous Poisson process (HPPP) is [12], where the probability density function (PDF) of the received signal at a point location was derived based on the assumption of white Gaussian transmit signals. Since the receiver size was negligible, the placement of transmitters did not need to accommodate the receiver's location. More importantly, only the Monte Carlo simulation, and not particle-based simulation, was performed to verify the derived PDF.

From the perspective of receiver type, many works have focused on the passive receiver, which can observe and count the number of molecules inside the receiver without interfering with the molecules [9, 12]. In nature, receivers commonly remove information molecules from the environment once they bind to a receptor. One example is the fully absorbing receiver, which absorbs all the molecules hitting its surface [10, 11]. However, no work has studied the channel characteristics and the received signal at the fully absorbing receiver in a large-scale molecular communication system, let alone its comparison with that at the passive receiver.

In this paper, we model the collective signal strength at the passive receiver and fully absorbing receiver due to a swarm of mobile point transmitters that simultaneously emit a given number of information molecules. Unlike [12], which focused on the statistics of the received signal at any point location, we focus on examining and deriving exact expressions for

the expected number of molecules observed inside two types of receiver for signal demodulation. This is achieved using stochastic geometry, which has been extensively used to model and provide simple and tractable results for wireless systems [13]. Our contributions can be summarized as follows:

1) We use stochastic geometry to model the collective signal at a receiver in a large-scale molecular communication system, where the receiver is either passive or fully absorbing. We distinguish between the desired signal due to the nearest transmitter and the interfering signal due to the other transmitters.
2) We derive a simple closed-form expression for the expected number of molecules absorbed at the fully absorbing receiver, and a tractable expression for the expected number of molecules observed inside the passive receiver at any time instant.
3) We define and derive tractable analytical expressions for the fraction of molecules due to the nearest transmitter and the fraction of molecules due to the other transmitters.
4) We verify our results using particle-based simulation and Monte Carlo simulation, which prove that the expected number of molecules observed at both types of receiver increases linearly with increasing transmitter density.

II. System Model

We consider a large-scale molecular communication system with a single receiver in which a swarm of point transmitters are spatially distributed outside the receiver in $\mathbb{R}^3/V_{\Omega_{r_r}}$ according to an independent and HPPP Φ with density λ, where $V_{\Omega_{r_r}}$ is the volume of receiver Ω_{r_r}. This spatial distribution, which was previously used to model wireless sensor networks [14], cellular networks [13] and heterogenous cellular networks [15], has also been applied to model bacterial colonies in [16] and the interference sources in a molecular communication system [12]. We consider a fluid environment in the absence of flow currents: the extension for flow currents will be treated in future work.

At any given time instant, a number of transmitters will be either silent or active. Thus, we define the activity probability of a transmitter that is triggered to transmit data as $\rho_a (0 < \rho_a < 1)$. This activity probability is independent of the receiver's location. Thus, the active point transmitters constitute independent HPPPs Φ_a with intensities $\lambda_a = \lambda\rho_a$. Each transmitter transmits molecular signal pulses with amplitude $N_{\text{tx}}^{\text{FA}}$ ($N_{\text{tx}}^{\text{PS}}$) to the absorbing receiver (the passive receiver). We assume the existence of a global clock such that all molecule emissions can only occur at $t = 0$.

We consider two types of spherical receiver with radius r_r: 1) Fully absorbing receiver [17], and 2) Passive receiver [4, 18]. To equivalently compare them, we assume both types of receiver are capable of counting the number of information molecules within the receiver volume at any time instant for information decoding.

It is well known that the distance between the transmitter and the receiver in molecular communication is the main contributor to the degradation of the signal strength (i.e., the number of molecules observed at the receiver). Instinctively, we assume that the receiver is associated with the nearest transmitter to obtain the strongest signal. Thus, the messenger molecules transmitted by other active point transmitters act as interference, which impairs the correct reception at the receiver. To measure this impairment, we formulate the desired signal, the interfering signal for the absorbing receiver and the passive receiver in the following subsections.

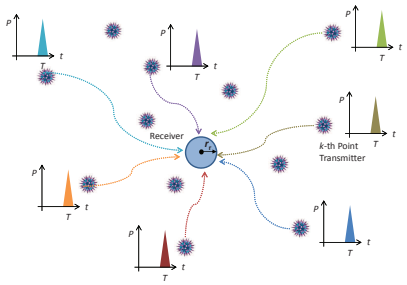

Fig. 1. Illustration of a receptor receiving molecular pulse signals from point transmitters at different distances.

A. Absorbing Receiver

In our proposed large-scale molecular communication system, let us consider the center of an absorbing receiver located at the origin. Using the Slivnyak-Mecke's theorem [13], the fraction F^{FA} of molecules absorbed at the receiver until time T due to an *arbitrary* point transmitter x at the location $\mathbf{x}$ with molecule emission occurring at $t = 0$ can be represented as [17]

$$F^{\text{FA}}\left(\Omega_{r_r}, T \middle| \|\mathbf{x}\|\right) = \frac{r_r}{\|\mathbf{x}\|} \operatorname{erfc}\left\{\frac{\|\mathbf{x}\| - r_r}{\sqrt{4DT}}\right\}, \tag{1}$$

where $\|\mathbf{x}\|$ is the distance between the point transmitter and the center of the receiver where the transmitters follow a HPPP, and D is the constant diffusion coefficient, which is usually obtained via experiment as in [19, Ch. 5]. The fraction F_{u}^{FA} of molecules absorbed inside the receiver until time T due to a single pulse emission by the *nearest* active transmitter can be represented as

$$F_{\text{u}}^{\text{FA}}\left(\Omega_{r_r}, T \middle| \|\mathbf{x}^*\|\right) = \frac{r_r}{\|\mathbf{x}^*\|} \operatorname{erfc}\left\{\frac{\|\mathbf{x}^*\| - r_r}{\sqrt{4DT}}\right\}, \tag{2}$$

where $\|\mathbf{x}^*\|$ denotes the distance between the receiver and the nearest transmitter,

$$x^* = \underset{x \in \Phi_a}{\arg\min} \|\mathbf{x}\|, \tag{3}$$

x^* denotes the nearest point transmitter for the receiver, and Φ_a denotes the set of active transmitters' positions.

The fraction of molecules absorbed at the receiver until time T due to single pulse emissions at each active interfering transmitter F_{I}^{FA} and that due to a single pulse emission at each

active transmitter $F_{\text{all}}^{\text{FA}}$ is represented as

$$F_{\text{I}}^{\text{FA}}\left(\Omega_{r_r},T|\left\|\mathbf{x}\right\|\right)=\sum_{\Phi_a/\mathbf{x}^*}\frac{r_r}{\left\|\mathbf{x}\right\|}\operatorname{erfc}\Big\{\frac{\left\|\mathbf{x}\right\|-r_r}{\sqrt{4DT}}\Big\},\quad(4)$$

and

$$F_{\text{all}}^{\text{FA}}\left(\Omega_{r_r},T|\left\|\mathbf{x}\right\|\right)=\sum_{\Phi_a}\frac{r_r}{\left\|\mathbf{x}\right\|}\operatorname{erfc}\Big\{\frac{\left\|\mathbf{x}\right\|-r_r}{\sqrt{4DT}}\Big\},\quad(5)$$

respectively.

The expected number of molecules absorbed at the receiver by time T due to all active transmitters is equivalently the expected number of molecules absorbed at the receiver until time T, which can be calculated as

$$\begin{aligned}\mathbb{E}\left\{N_{\text{all}}^{\text{FA}}\left(\Omega_{r_r},T\right)\right\}&=N_{\text{tx}}^{\text{FA}}F_{\text{all}}^{\text{FA}}\left(\Omega_{r_r},T|\left\|\mathbf{x}\right\|\right)\\&=\underbrace{N_{\text{tx}}^{\text{FA}}F_{\text{u}}^{\text{FA}}\left(\Omega_{r_r},T|\left\|\mathbf{x}^*\right\|\right)}_{\mathbb{E}_{\text{u}}^{\text{FA}}}+\underbrace{N_{\text{tx}}^{\text{FA}}F_{\text{I}}^{\text{FA}}\left(\Omega_{r_r},T|\left\|\mathbf{x}\right\|\right)}_{\mathbb{E}_{\text{I}}^{\text{FA}}},\end{aligned}\quad(6)$$

where $F_{\text{all}}^{\text{FA}}\left(\Omega_{r_r},T|\left\|\mathbf{x}\right\|\right)$ is given in (5), $\mathbb{E}_{\text{u}}^{\text{FA}}$ is the fraction of absorbed molecules at the absorbing receiver until time T due to the nearest transmitter, and $\mathbb{E}_{\text{I}}^{\text{FA}}$ is the fraction of absorbed molecules at the absorbing receiver until time T due to the other (interfering) transmitters.

B. Passive Receiver

In a point-to-point molecular communication system with a single point transmitter located distance $\left\|\mathbf{x}\right\|$ away from the center of a passive receiver with radius r_r, the local point concentration at the center of the passive receiver at time T due to a single pulse emission by the transmitter is given as [20, Eq. (4.28)]

$$C\left(\Omega_{r_r},T|\left\|\mathbf{x}\right\|\right)=\frac{1}{\left(4\pi DT\right)^{3/2}}\exp\Big(-\frac{\left\|\mathbf{x}\right\|^2}{4DT}\Big).\quad(7)$$

The fraction of information molecules observed inside the passive receiver with volume $V_{\Omega_{r_r}}$ at time T is denoted as

$$F^{\text{PS}}\left(\Omega_{r_r},T|\left\|\mathbf{x}\right\|\right)=\int\limits_{V_{\Omega_{r_r}}}C\left(\Omega_{r_r},T|\left\|\mathbf{x}\right\|\right)dV_{\Omega_{r_r}},\quad(8)$$

where $V_{\Omega_{r_r}}$ is the volume of the spherical passive receiver.

According to (8) and Theorem 2 in [21], the fraction F^{PS} of information molecules observed inside the passive receiver at time T due to a single pulse emission by a transmitter at time t is derived as

$$\begin{aligned}F^{\text{PS}}\left(\Omega_{r_r},T|\left\|\mathbf{x}\right\|\right)&=\frac{1}{2}\left[\operatorname{erf}\Big(\frac{r_r-\left\|\mathbf{x}\right\|}{2\sqrt{DT}}\Big)+\operatorname{erf}\Big(\frac{r_r+\left\|\mathbf{x}\right\|}{2\sqrt{DT}}\Big)\right]\\&+\frac{\sqrt{DT}}{\sqrt{\pi}\left\|\mathbf{x}\right\|}\left[\exp\Big(-\frac{\left(r_r+\left\|\mathbf{x}\right\|\right)^2}{4DT}\Big)-\exp\Big(-\frac{\left(\left\|\mathbf{x}\right\|-r_r\right)^2}{4DT}\Big)\right],\end{aligned}\quad(9)$$

which does *not* assume that the molecule concentration inside the passive receiver is uniform. This is unlike the common assumption that the concentration of molecule inside the passive receiver is uniform. Although that assumption is commonly applied, it relies on the receiver being sufficiently far from the transmitter (see [21]), which we cannot guarantee here since the transmitters are placed randomly.

In the large-scale molecular communication system with a passive receiver centered at the origin, the expected number of molecules observed inside the receiver at time T due to a single pulse emission at *all* active transmitters at $t=0$ is given as

$$\begin{aligned}\mathbb{E}\left\{N_{\text{all}}^{\text{PS}}\left(\Omega_{r_r},T\right)\right\}&=\mathbb{E}\left\{\sum_{\Phi_a}N_{\text{tx}}^{\text{PS}}F^{\text{PS}}\left(\Omega_{r_r},T|\left\|\mathbf{x}\right\|\right)\right\}\\&=\underbrace{N_{\text{tx}}^{\text{PS}}F_{\text{u}}^{\text{PS}}\left(\Omega_{r_r},T|\left\|\mathbf{x}^*\right\|\right)}_{\mathbb{E}_{\text{u}}^{\text{PS}}}+\underbrace{N_{\text{tx}}^{\text{PS}}F_{\text{I}}^{\text{PS}}\left(\Omega_{r_r},T|\left\|\mathbf{x}\right\|\right)}_{\mathbb{E}_{\text{I}}^{\text{PS}}},\end{aligned}\quad(10)$$

where $F^{\text{PS}}\left(\Omega_{r_r},T|\left\|\mathbf{x}\right\|\right)$ is given in (9), $\mathbb{E}_{\text{u}}^{\text{PS}}$ is the fraction of molecules observed inside the receiver at time T due to the nearest transmitter, and $\mathbb{E}_{\text{I}}^{\text{PS}}$ is the fraction of molecules observed inside the receiver at time T due to the other (interfering) transmitters.

III. Receiver Observations

In this section, we first derive the distance distribution between the receiver and the nearest point transmitter. By doing so, we derive exact expressions for the expected number of molecules observed inside the receiver due to the nearest point transmitter and that due to the interfering transmitters.

A. Distance Distribution

Unlike the stochastic geometry modelling of wireless networks, where the transmitters are randomly located in the unbounded space, the point transmitters in a large-scale molecular communication system can only be distributed *outside* the surface of the spherical receiver. Taking into account the minimum distance r_r between point transmitters and the receiver center, we derive the probability density function (PDF) of the shortest distance between a point transmitter and the receiver in the following proposition.

Proposition 1. *The PDF of the shortest distance between any point transmitter and the receiver in 3D space is given by*

$$f_{\left\|x^*\right\|}(x)=4\lambda_a\pi x^2e^{-\lambda_a\left(\frac{4}{3}\pi x^3-\frac{4}{3}\pi {r_r}^3\right)},\quad(11)$$

where $\lambda_a=\lambda\rho_a$.

Proof. See Appendix A. □

Based on the proof of Proposition 1, we also derive the PDF of the shortest distance between any point transmitter and the receiver in 2D space in the following lemma.

Corollary 1. *The PDF of the shortest distance between any point transmitter and the receiver in 2D space is given by*

$$f_{\left\|x^*\right\|}(x)=2\lambda_a\pi re^{-\lambda_a\left(\pi r^2-\pi {r_r}^2\right)},\quad(12)$$

where $\lambda_a=\lambda\rho_a$.

B. Absorbing Receiver Observations

In this subsection, we derive a closed-form expression for the expected number of molecules observed inside the absorbing receiver in 3D space.

Using Campbell's theorem, we derive the expected number of absorbed molecules due to the nearest transmitter and that due to the interfering transmitters until time t as

$$\mathbb{E}_{\mathrm{u}}^{\mathrm{FA}} = N_{\mathrm{tx}}^{\mathrm{FA}} \int_{r_r}^{\infty} \Pi_0^t(x)\, 4\lambda_a \pi x^2 e^{-\lambda_a\left(\frac{4}{3}\pi x^3 - \frac{4}{3}\pi {r_r}^3\right)} dx, \quad (13)$$

and

$$\mathbb{E}_{\mathrm{I}}^{\mathrm{FA}} = N_{\mathrm{tx}}^{\mathrm{FA}} (4\pi\lambda_a)^2 \int_{r_r}^{\infty}\int_{x}^{\infty} \Pi_0^t(r) r^2 dr x^2 e^{-\lambda_a\left(\frac{4}{3}\pi x^3 - \frac{4}{3}\pi {r_r}^3\right)} dx, \quad (14)$$

respectively.

Theorem 1. *The expected net number of molecules absorbed at the absorbing receiver in 3D space during any sampling time interval $[t, t+T_{ss}]$ is derived as*

$$\mathbb{E}\left\{N_{\mathrm{all}}^{\mathrm{FA}}(\Omega_{r_r}, t, t+T_{ss})\right\} = 4N_{\mathrm{tx}}^{\mathrm{FA}}\sqrt{\pi}\lambda_a r_r \left[D\sqrt{\pi}T_{ss} + 2\sqrt{D} r_r \left(\sqrt{T_{ss}+t} - \sqrt{t}\right)\right]. \quad (15)$$

The expected number of molecules observed inside the fully absorbing receiver in 3D space until time t is derived as

$$\mathbb{E}\left\{N_{\mathrm{all}}^{\mathrm{FA}}(\Omega_{r_r}, t)\right\} = 4N_{\mathrm{tx}}^{\mathrm{FA}}\sqrt{\pi}\lambda_a r_r \left[D\sqrt{\pi}t + 2r_r\sqrt{Dt}\right]. \quad (16)$$

Proof. See Appendix B. □

From Theorem 1, we find that the expected number of molecules absorbed at the absorbing receiver at time t is linearly proportional to the density of active transmitters, and increases with increasing diffusion coefficient or receiver radius. As expected, we find that the expected number of molecules absorbed at the receiver until t is always increasing with time t.

C. Passive Receiver Observations

In the following theorem, we derive the expected number of molecules observed inside the passive receiver in 3D space.

Using Campbell's theorem, we derive the expected number of observed molecules due to the nearest transmitter and that due to the interfering transmitters at time t as

$$\mathbb{E}_{\mathrm{u}}^{\mathrm{PS}} = 4\lambda_a \pi N_{\mathrm{tx}}^{\mathrm{PS}} e^{\frac{4}{3}\pi {r_r}^3 \lambda_a} \int_{r_r}^{\infty} \Phi(x)\, x^2 \exp\left\{-\frac{4}{3}\pi x^3 \lambda_a\right\} dx, \quad (17)$$

and

$$\mathbb{E}_{\mathrm{I}}^{\mathrm{PS}} = (4\pi\lambda_a)^2 e^{\frac{4}{3}\pi {r_r}^3\lambda_a} N_{\mathrm{tx}}^{\mathrm{PS}} \int_{r_r}^{\infty}\int_{x}^{\infty} \Phi(r) r^2 dr\, x^2 e^{-\frac{4}{3}\pi x^3 \lambda_a} dx, \quad (18)$$

respectively. In (17) and (18), $\Phi(r) = F^{\mathrm{PS}}(\Omega_{r_r}, t|\, r)$.

Theorem 2. *The expected net number of molecules observed inside the passive receiver during any sampling time interval $[t, t+T_{ss}]$ in 3D space is derived as*

$$\mathbb{E}\left\{N_{\mathrm{all}}^{\mathrm{PS}}(\Omega_{r_r}, t, t+T_{ss}|\, \|\mathbf{x}\|)\right\} = 4N_{\mathrm{tx}}^{\mathrm{PS}}\pi\lambda_a \left[\int_{r_r}^{\infty} F^{\mathrm{PS}}(\Omega_{r_r}, t+T_{ss}|\, r) r^2 dr - \int_{r_r}^{\infty} F^{\mathrm{PS}}(\Omega_{r_r}, t|\, r) r^2 dr\right], \quad (19)$$

where $F^{\mathrm{PS}}(\Omega_{r_r}, t|\, r)$ is given in (9)*.*

The expected number of molecules observed inside the passive receiver at time t in 3D space is derived as

$$\mathbb{E}\left\{N_{\mathrm{all}}^{\mathrm{PS}}(\Omega_{r_r}, 0, t|\, \|\mathbf{x}\|)\right\} = 4N_{\mathrm{tx}}^{\mathrm{PS}}\pi\lambda_a \int_{r_r}^{\infty} F^{\mathrm{PS}}(\Omega_{r_r}, t|\, r) r^2 dr. \quad (20)$$

Proof. Analogous to Appendix B without solving the integrals. □

In Theorem 2, we observe that the expected number of molecules observed inside the passive receiver also increases proportionately with the density of active transmitters.

IV. Numerical and Simulation Results

In this section, we examine the expected number of molecules observed at the absorbing receiver and the passive receiver due to simultaneous single pulse emissions at all active point transmitters. In all figures of this section, we set the parameters as follows: $r_r = 5\,\mu$m and $N_{\mathrm{tx}}^{\mathrm{FA}} = N_{\mathrm{tx}}^{\mathrm{PS}} = 10^4$. In all figures, the analytical curves of the expected number of molecules absorbed at the absorbing receiver due to all the transmitters, the nearest transmitter, and the interfering transmitters are plotted using Eqs. (15), (13), and (14), and are abbreviated as "Absorbing All", "Absorbing Nearest", and "Absorbing Aggregate", respectively. The analytical curves of the expected number of molecules observed inside the passive receiver due to all the transmitters, the nearest transmitter, the interfering transmitters are plotted using (19), (17), and (18), and are abbreviated as "Passive All", "Passive Nearest", and "Passive Aggregate", respectively.

A. Particle-Based and Pseudo Simulation Validation

In Fig. 2, we set $D = 80 \times 10^{-12}\,\frac{\mathrm{m}^2}{\mathrm{s}}$, and assume that the transmitters are placed up to $R = 50\,\mu$m from the center of the receiver at a density of $\lambda_a = 10^{-4}$ transmitters per $\mu\mathrm{m}^3$ (i.e., 52 average number of transmitters, including the subtraction of the receiver volume). The receiver takes samples every $T_{ss} = 0.01$ s and calculates the net change in the number of observed molecules between samples. The default simulation time step is also 0.01 s. Unless otherwise noted, all simulation results were averaged over 10^4 transmitter location permutations, with each permutation simulated at least 10 times.

In Fig. 2, we verify the analytical expressions for the expected net number of molecules observed during $[t, t+T_{ss}]$ at the absorbing receiver in Eq. (13) and Eq. (14), and that inside the passive receiver in Eq. (17) and Eq. (18) by comparing with the particle-based simulations and the Monte Carlo

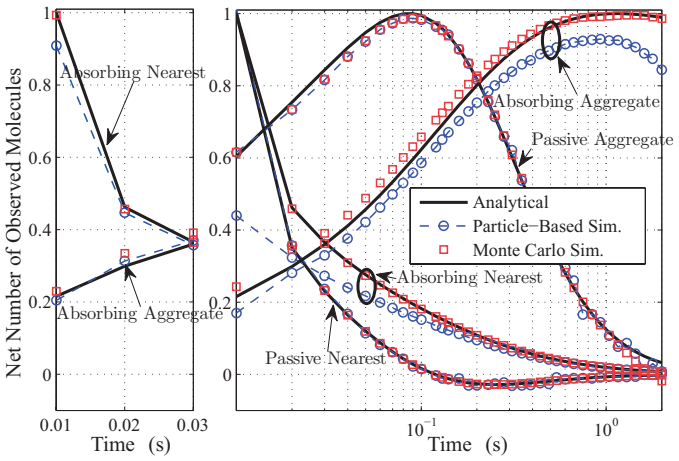

Fig. 2. Net number of observed molecules inside the receiver as a function of time. All curves are scaled by the maximum value of the analytical curves in the right subplot.

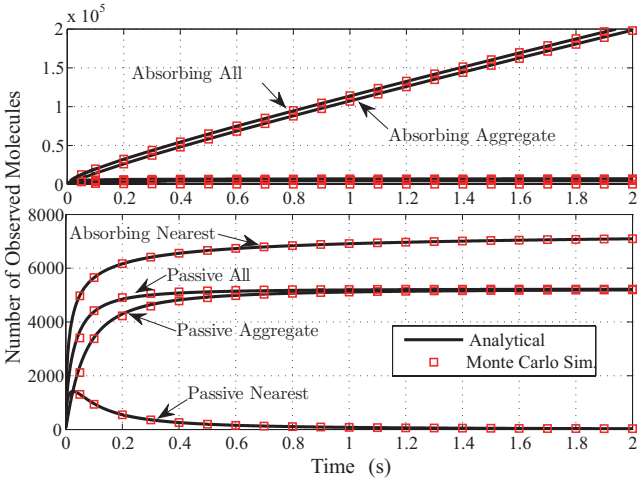

Fig. 3. Expected number of molecules observed inside the receiver as a function of time.

TABLE II
THE SIMULATION PARAMETERS AND SCALING VALUES APPLIED IN FIG. 2.

Transmitter	Receiver	Realizations	Time Step [s]	Scaling Value
Nearest	Passive	10^4	10^{-2}	149.57
Nearest	Active	10^4	10^{-2}	354.52
Aggregate	Passive	10^4	10^{-2}	9.252
Aggregate	Active	10^3	10^{-3}	59.42

simulations. The particle-based simulations were performed by tracking the progress of individual particles to obtain the net number of observed molecules during $[t, t + T_{ss}]$ using the AcCoRD simulator (Actor-based Communication via Reaction-Diffusion) [22]. The pseudo simulations rely on the Monte Carlo simulation method, which were performed by averaging the expected number of observed molecules due to all active transmitters with randomly-generated location, as calculated from Eq. (1) and Eq. (9), over 10^4 realizations.

In the right subplot of Fig. 2, we compare passive and absorbing receivers and observe the expected net number of observed molecules during $[t, t+T_{ss}]$ due to the nearest transmitter and due to the aggregation of the interfering transmitters. In the left subplot of Fig. 2, we lower the simulation time step to 10^{-4} s for the first few samples of the two absorbing receiver cases, in order to demonstrate the corresponding improvement in accuracy. All curves in both subplots are scaled by the maximum value of the corresponding analytical curve in the right subplot; the scaling values and other simulation parameters are summarized in Table II.

1) Particle-Based Simulation Validation: Overall, there is good agreement between the analytical curves and the particle-based simulations in the right subplot of Fig. 2. The analytical results for the net number of molecules observed inside the passive receiver during $[t, t+T_{ss}]$ due to the nearest transmitter is highly accurate, and even captures the net loss of molecules observed after $t = 0.1$ s. There is a slight deviation in the particle-based simulation for the "passive aggregate" curve, particularly as time approaches $t = 1$ s, which is primarily due to the very low number of molecules observed at this time (note that the scaling factor in this case is only 9.252; see Table II).

There is less agreement between the particle-based simulations and the analytical expressions for the absorbing receiver, and this is primarily due to the large simulation time step (even though we used a smaller time step for the aggregate transmitter case in the right subplot; see Table II). To demonstrate the impact of the time step, the left subplot shows much better agreement for the absorbing receiver model by lowering the time step to 10^{-4} s. This improvement is especially true in the case of the nearest transmitter, as there is significant deviation between the particle-based simulation and the analytical expression for very early times in the right subplot.

2) Monte Carlo Simulation Validation: There is a good match between the analytical curves and the Monte Carlo simulations for the net number of molecules observed at both types of receiver during $[t, t+T_{ss}]$ due to the nearest transmitter, which can be attributed to the large number of molecules and the shortest distance value compared with $R = 50\,\mu$m (as shown in Table II). There is slight deviation in the Monte Carlo simulations for the expected number of molecules observed inside both types of receiver due to the interfering transmitters, and this is primarily due to the restricted placement of transmitters to the maximum distance $R = 50\,\mu$m. In Figs. 3, better agreement between the analytical curves and pseudo simulation is achieved by increasing the maximum placement distance R.

Due to the extensive computational demands to simulate such large molecular communication environments, we assume that the particle-based simulations have sufficiently verified the analytical models. The remaining simulation results in Fig. 3 is only generated via Monte Carlo simulation.

B. Performance Evaluation

From Fig. 2 and the scaling values in Table II, we see that the expected net number of molecules absorbed at the absorbing receiver is much larger than that inside the passive receiver, since every molecule arriving at the absorbing receiver is permanently absorbed. We also notice that the expected net number of absorbed molecules due to the nearest transmitter is much larger than that due to the interfering transmitters, which may be due to a relatively low transmitter density.

Interestingly, the concurrent single pulse transmission by the transmitters at time $t = 0$ results in a longer and stronger channel response at the absorbing receiver than that at the passive receiver. If the demodulation is based on the number of observed molecules during each bit interval, the longer channel response at the absorbing receiver may contribute to higher ISI than at a passive receiver for the same bit interval, whereas its stronger channel response may benefit signal detection.

In Fig. 3, we set the parameters: $D = 120 \times 10^{-12} \frac{\mathrm{m}^2}{\mathrm{s}}$, $R = 100\,\mu\mathrm{m}$, and $T_{ss} = 0.1$ s. Fig. 3 plots the expected number of molecules observed at the absorbing receiver and the passive receiver at time t. We set the density of active transmitters as $\lambda_a = 10^{-3}/\mu\mathrm{m}^3$. As shown in the lower subplot of Fig. 3, the channel responses of the receivers due to the nearest transmitter in this large-scale molecular communication system are consistent with those observed at the absorbing receiver in [11, Fig. 4] and the passive receiver in [4, Fig. 2] and [18, Fig. 1] for a point-to-point molecular communication system.

In Fig. 3, we notice that the expected number of observed molecules at time t due to all the transmitters is dominated by the interfering transmitters, rather than the nearest transmitter, which is due to the higher density of transmitters. Furthermore, as we might expect, the expected number of molecules observed inside the passive receiver at time t stabilizes after $t = 0.8\,\mathrm{s}$, whereas that at the absorbing receiver increases linearly with increasing time. This reveals the potential differences in optimal demodulation and interference cancellation design for these two types of receiver.

V. Conclusions and Future Work

In this paper, we provided a general model for the transmitter modelling in a large-scale molecular communication system using stochastic geometry. The collective signal strength at a fully absorbing receiver and a passive receiver are modelled and examined. We derived tractable expressions for the expected number of observed molecules at the fully absorbing receiver and the passive receiver, which were shown to increase with transmitter density. Our analytical results were validated through particle-based simulation and Monte Carlo simulation. The analytical model presented in this paper can also be applied for the performance evaluation of other types of receiver (e.g., partially absorbing, reversible adsorption receiver, ligand-binding receiver) in large-scale molecular communication systems by substituting its corresponding channel response.

References

[1] T. Nakano, A. Eckford, and T. Haraguchi, *Molecular communication*. Cambridge University Press, 2013.

[2] E. Codling, M. Plank, and S. Benhamous, "Random walk models in biology," *Journal of The Royal Society Interface*, vol. 5, no. 25, pp. 813–834, Aug. 2008.

[3] S. Atkingson and P. Williams, "Quorum sensing and social networking in the microbial world," *Journal of The Royal Society Interface*, vol. 6, no. 40, pp. 959–978, Aug. 2009.

[4] I. Llatser, A. Cabellos-Aparicio, and M. Pierobon, "Detection techniques for diffusion-based molecular communication," *IEEE Journal on Selected Areas in Communications (JSAC)*, vol. 31, pp. 726–734, Dec. 2013.

[5] W. Guo, C. Mias, N. Farsad, and J. Wu, "Molecular versus electromagnetic wave propagation loss in macro-scale environments," *IEEE Trans. Mol. Biol. Multi-Scale Commun.*, vol. 1, Mar. 2015.

[6] S. M. Douglas, I. Bachelet, and G. M. Church, "A logic-gated nanorobot for targeted transport of molecular payloads," *Science*, vol. 335, no. 6070, pp. 831–834, Feb. 2012.

[7] A. Cavalcanti, T. Hogg, B. Shirinzadeh, and H. Liaw, "Nanorobot communication techniques: a comprehensive tutorial," in *Proc. IEEE Int. Conf. Control, Autom., Robot., Vis.*, Dec. 2006, pp. 1–6.

[8] C. J. Kirkpatrick and W. Bonfield, "Nanobiointerface: a multidisciplinary challenge," *Journal of The Royal Society Interface*, vol. 7, no. Suppl 1, pp. S1–S4, Dec. 2009.

[9] A. Noel, K. C. Cheung, and R. Schober, "A unifying model for external noise sources and isi in diffusive molecular communication," *IEEE J. Sel. Areas Commun.*, vol. 32, no. 12, pp. 2330–2343, Dec 2014.

[10] H. B. Yilmaz and C.-B. Chae, "Simulation study of molecular communication systems with an absorbing receiver: Modulation and ISI mitigation techniques," *Simulat. Modell. Pract. Theory*, vol. 49, pp. 136–150, Dec. 2014.

[11] Y. Deng, A. Noel, M. Elkashlan, A. Nallanathan, and K. C. Cheung, "Modeling and simulation of molecular communication systems with a reversible adsorption receiver," *arXiv*, 2016. [Online]. Available: http://arxiv.org/abs/1601.00681

[12] M. Pierobon and I. F. Akyildiz, "A statistical–physical model of interference in diffusion-based molecular nanonetworks," *IEEE Trans. Commun.*, vol. 62, no. 6, pp. 2085–2095, Jun. 2014.

[13] F. Baccelli and B. Blaszczyszyn, *Stochastic geometry and wireless networks: Volume 1: Theory*. Now Publishers Inc, 2009, vol. 1.

[14] Y. Deng, L. Wang, M. Elkashlan, A. Nallanathan, and R. K. Mallik, "Physical layer security in three-tier wireless sensor networks: A stochastic geometry approach," *IEEE Trans. Inf. Forensics Security*, vol. 11, no. 6, pp. 1128–1138, Jun. 2016.

[15] Y. Deng, L. Wang, M. Elkashlan, M. Direnzo, and J. Yuan, "Modeling and analysis of wireless power transfer in heterogeneous cellular networks," *IEEE Trans. Commun.*, 2016.

[16] S. Jeanson, J. Chadoeuf, M. Madec, S. Aly, J. Floury, T. F. Brocklehurst, and S. Lortal, "Spatial distribution of bacterial colonies in a model cheese," *Applied and Environmental Microbiology*, vol. 77, no. 4, pp. 1493–1500, Dec. 2010.

[17] H. B. Yilmaz, A. C. Heren, T. Tugcu, and C.-B. Chae, "Three-Dimensional channel characteristics for molecular communications with an absorbing receiver," *IEEE Communications Letters*, vol. 18, no. 6, pp. 929–932, Jun. 2014.

[18] A. Noel, K. C. Cheung, and R. Schober, "Improving receiver performance of diffusive molecular communication with enzymes," *IEEE Trans. Nanobiosci.*, vol. 13, no. 1, pp. 31–43, Mar. 2014.

[19] E. L. Cussler, *Diffusion: mass transfer in fluid systems*. Cambridge university press, 2009.

[20] P. Nelson, *Biological Physics: Energy, Information, Life*, updated 1st ed. W. H. Freeman and Company, 2008.

[21] A. Noel, K. C. Cheung, and R. Schober, "Using dimensional analysis to assess scalability and accuracy in molecular communication," in *Proc. IEEE ICC MoNaCom*, Jun. 2013, pp. 818–823.

[22] A. Noel. (2016) Actor-based communication via reaction-diffusion. [Online]. Available: https://github.com/adamjgnoel/AcCoRD